DISTRIBUTION STATEMENT A. Approved for public release; distribution is unlimited.

Sediment Flux and Trapping on the Skagit Tidal Flats: Analysis and Modeling

David K. Ralston
Applied Ocean Physics and Engineering, MS #12
Woods Hole, MA 02543
phone: (508) 289-2587 fax: (508) 457-2194 email: dralston@whoi.edu

W. Rockwell Geyer
Woods Hole Oceanographic Institution, MS 11
Woods Hole, MA 02543
phone: 508-289-2868 fax: 508-457-2194 email: rgeyer@whoi.edu

Peter Traykovski
MS 12, Woods Hole Oceanographic Institution
Woods Hole, MA 02543
phone: 508-289-2638 fax: 508-457-2194 ptraykovski@whoi.edu

Award Number: N00014-10-1-0253

LONG-TERM GOALS

The long-term objective is to determine the hydrodynamic processes controlling sediment transport and the associated morphologic response on tidal flats.

OBJECTIVES

The objectives of this project are to analyze the data from the Skagit Flats deployment of June, 2009 and complete several papers that document our findings. The themes of analysis are

- to ascertain the influence of freshwater inflow on the barotropic and baroclinic dynamics of Skagit Flats, and then to ascertain their consequences for sediment transport and trapping;
- to determine the processes causing tidal and high-frequency (up to surface gravity-wave frequency) variations in bottom stress, turbulence and suspended sediment concentrations, including the possible formation and destruction of fluid mud layers and episodes of rapid sediment accumulation and erosion;
- to quantify the mechanisms causing tidal asymmetry in bottom stress and sediment transport rate on Skagit Flats and determine the implications of these asymmetries for the sediment balance and morphological structure of the flats.

APPROACH

To investigate sediment fluxes on fluvial tidal flats we have coupled detailed field observations with a high resolution numerical model of the hydrodynamics and sediment transport. The observations were made on the Skagit Tidal flats in Puget Sound as part of the Tidal Flats DRI, and that effort included collaboration and sharing of data with other investigators in the DRI. The numerical model was developed and refined based on comparisons with observations. The project is currently in an analysis phase using both the field observations and results from the calibrated model simulations.

WORK COMPLETED

During June, 2009, an intensive field campaign with fixed and shipboard observations was conducted on Skagit Flats (Fig. 1). The fixed array included seven intensively instrumented stations on the flats and five water-level stations within the distributaries of the Skagit River. Quad-pods were deployed at five of the tidal flats stations, on which were mounted newly developed pulse-coherent acoustic Doppler profilers (pcADPs) as well as acoustic backscatter sensors (ABSs), conventional acoustic Doppler velocimeters (ADVs). All of flats stations included acoustic Doppler current profilers (ADCPs) and temperature-salinity sensors at multiple levels, as well as bottom pressure sensors.

Shipboard measurements included salinity-temperature-optical backscatter profiles and continuous ADCP and bathymetric measurements from a shallow-draft vessel during June 1-5 and June 22-26, 2009. Water samples were obtained under varying flow and turbidity conditions to provide calibration for the optical and acoustic turbidity sensors.

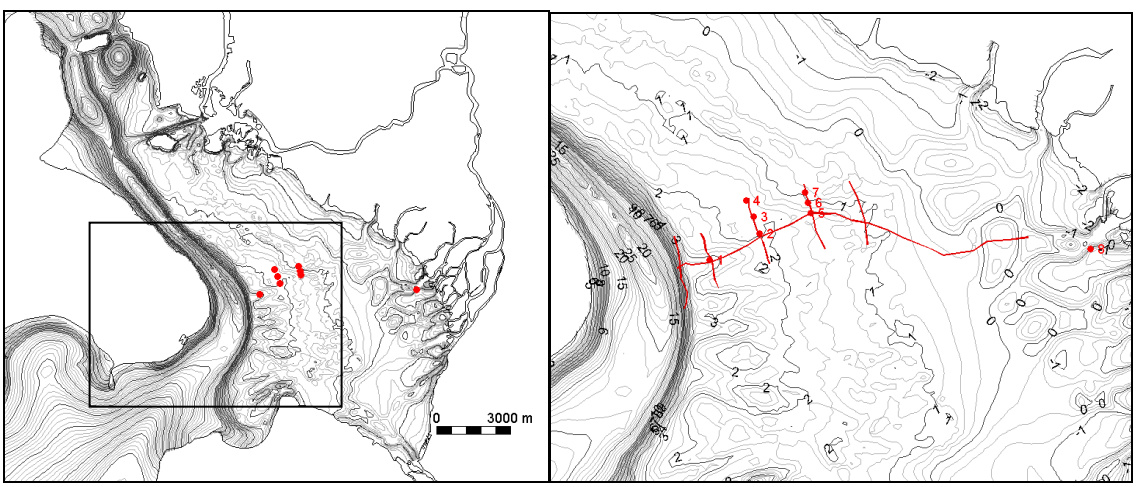

Figure 1. Bathymetry of the Skagit Bay tidal flats (left) with a zoom on the study area on the southern flats (right). Red dots indicate frame locations and lines show across-flats and across-channel survey lines.

During June 2009, the river discharge ranged from its year-to-date maximum of 930 $m^3 s^{-1}$ in early June to about 450 $m^3 s^{-1}$ by the end of the month. The observation period spanned two spring tides and a neap, with stronger spring tides occurring around the solstice. The maximum tidal range was 5 m and resulted in tidal currents reaching 1.2 m/s on June 24, while the minimum range was 2.5 m on June 15. Winds were generally light (mean wind speed 2.4 m/s; maximum 9 m/s on June 24). However there were periods of significant surface wave orbital motion, and there was a clear influence of tidal

currents on the wave amplitude. Suspended sediment concentrations were generally low to moderate, except during peak spring tides, when significant resuspension of sand occurred. During the early high-flow period, there was a distinctive wash load in the surface layer. Suspended sediment concentrations were calculated from acoustic and optical instruments based on calibrations with water samples collected during surveys.

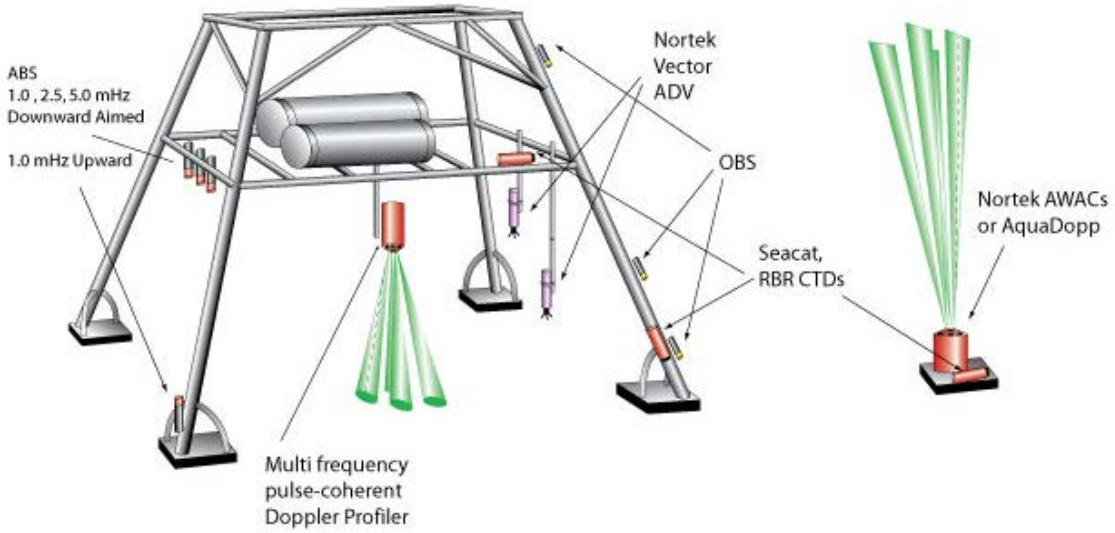

Figure 2. Schematic of a quadpod deployed at stations 1, 2, 3, 5 and 6 in Fig. 1 showing a typical equipment configuration. Each quadpod was accompanied by a upward looking acoustics Doppler current profiler (ADCP) and a bottom mounted conductivity-temperature-pressure sensor. Stations 4, 7 and 8 had only ADCP, CT, and pressure sensors.

Extensive efforts have gone into development of a high-resolution numerical of the Skagit tidal flats and surrounding region. Bathymetry was collected from multiple sources and combined to create an unstrucutred model grid. Grid resolution ranged from about 10 m on the flats in the study region to over 500 m in more distant parts of the domain. The bathymetry and grid in the distributary network of the Skagit were refined basd on surveys of depth and discharge in the river during the June 2009 obsevations. Data for boundary forcing of tides, river discharge, and winds were aquired and input into the model. In addition to the grid and forcing, the hydrodynamic code (FVCOM) had to be modified and tested for this implemetnation. A sediment transport module that incorporates the latest verion of the CSTMS has been implemented into FVCOM, and simulations have been run for test cases and for the Skagit domain. FVCOM was also modified to incorporate the most recent version of the Generalized Ocean Turbulence Model (GOTM), allowing application of different turbulent closure schemes and parameters to the simulations than then default Mellor-Yamada scheme. The flexibility to evaluate different turbulence closures is particular important in a highly stratified environments like the Skagit and for sediment transport calcuations that are sensitive to the calcuation of near-bed turbulence.

Two manuscript were written and submitted based on observations analyzed in this project, and are currently in review. Topics included an analyses of mechanisms for generating tidal asymmetries on the tidal flats (Nidzieko and Ralston) and an integration of model and observations quantifying impacts

of estuarine and fluvial process on sediment fluxes (Ralston et al.). An additional manuscript on the role of tidal straining for stratification dynamics on the tidal flats is in preparation.

RESULTS

The role of fresh water input to tidal flats on flow dynamics and sediment transport has received little attention to date. On tidal flats without significant river input, tidal and wave processes dominate the dynamical and sediment balances. However, the Skagit River supplies buoyancy and suspended sediment to the tidal flats of Skagit Bay. The freshwater flow creates strong stratification that increases velocity shear and reduces turbulent stresses. The stratification modulates with changes in river discharge, over spring-neap periods with changes in tidal amplitude, and at diurnal time scales with the wetting and drying of the flats.

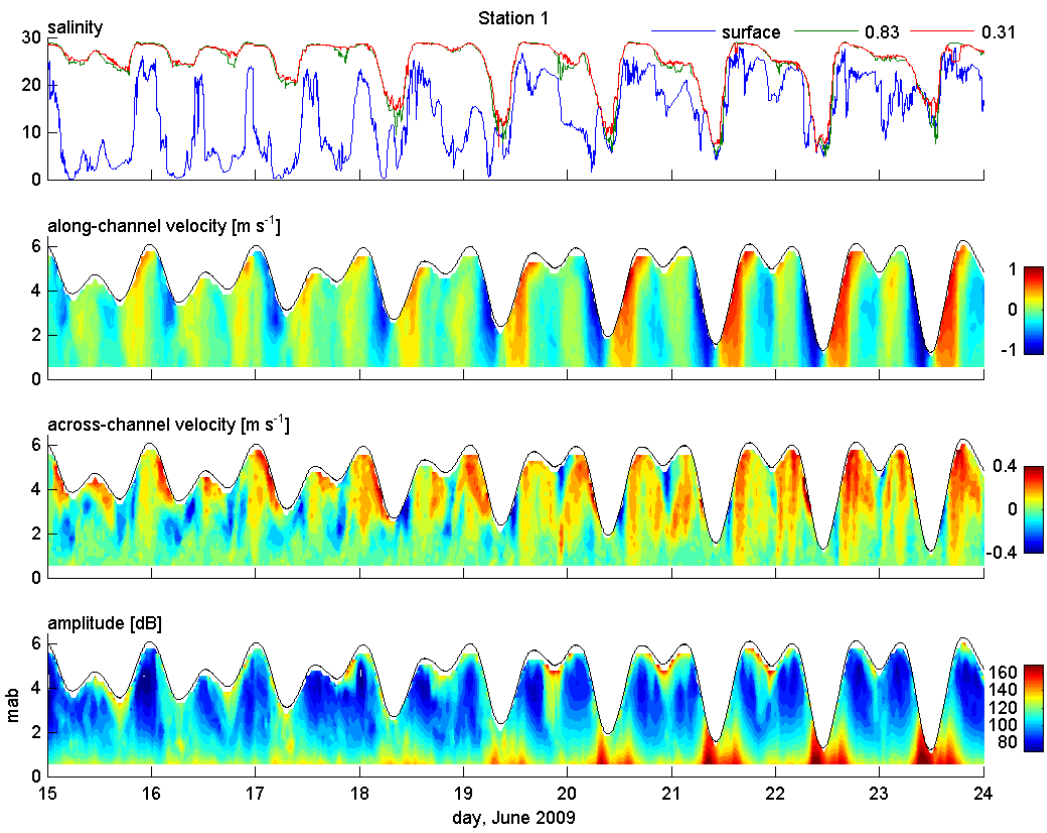

Figure 3. Time series of salinity, along-channel velocity, across-channel velocity, and acoustic backscatter at station 1 (location shown in Fig. 1) during the transition from neap to spring tides. Backscatter intensity is shown as a proxy for suspended sediment; optical backscatter sensors show similar spring-neap and tidal variability.

Suspended sediment dynamics and stratified turbulence

An example of the magnitude and variability of the stratification is shown for station 1 on the lower flats (Fig. 3), but similar conditions were observed at the other stations. The period shown is the

transition from neap to spring. During neap tides, stratification remained strong for most of each tidal cycle, with surface-to-bottom differences of ~25 psu. As tidal amplitudes and velocities increased, stratification decreased. Suspended sediment concentrations, as seen in acoustic and optical backscatter, also depended on tidal amplitude. Suspended sediment concentrations (SSC) remained low through the neap tides, but increased substantially spring ebb tides (e.g., days 20-23). Early in each strong ebb, stratification remained strong and SSC was low. The water column mixed as the tide approached low water at the same time that bottom stress and sediment concentrations increased significantly. SSC remained high and the water column was mixed or weakly stratified until midway through the subsequent strong floods. Suspended sediment concentrations decreased when the water column restratified mid-flood, and the near-surface velocity became strongly sheared.

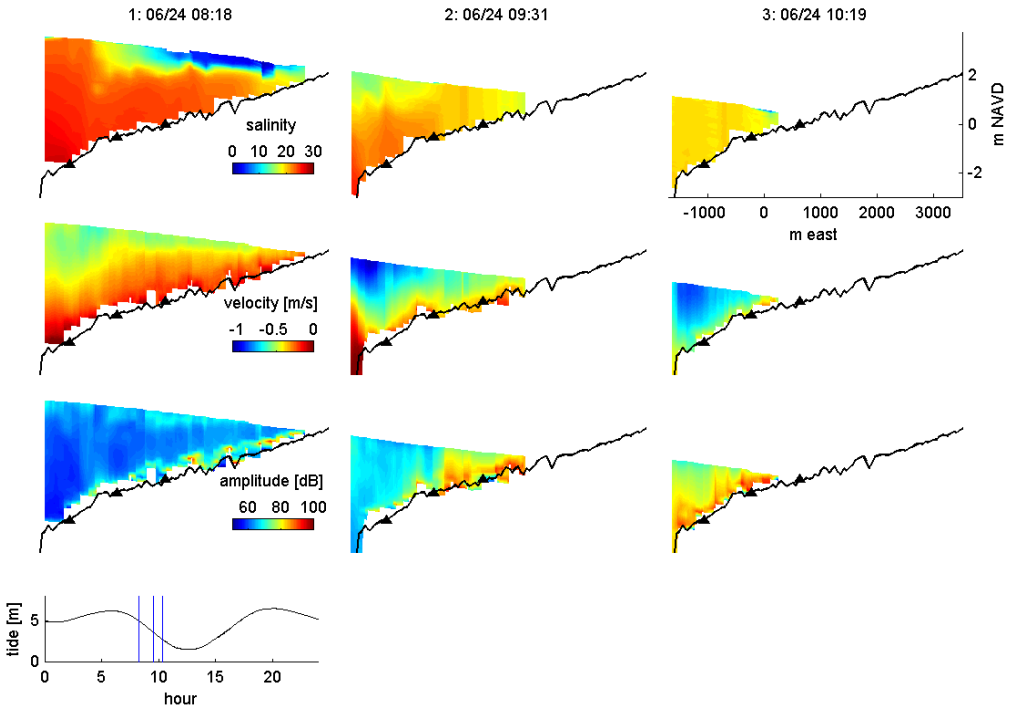

Figure 4. Three across-flats surveys of salinity (top), velocity (middle), and acoustic backscatter (bottom) during a spring ebb tide. Tidal elevation is in the lower left with survey times shown; stations 1, 2, and 5 are marked with triangles on the transects. The sloping water surface reflects the change in tidal elevation during each transect. In transect 1, strong stratification, strong velocity shear, and low acoustic backscatter extended across most of the flats. In transect 2, stratification remained strong on the lower flats (west of station 2), but on the upper flats the water column was vertically mixed, had less shear, and had higher backscatter. By transect 3, the well-mixed, high-backscatter region extended to the edge of the flats. This breakdown of stratification and increase in backscatter was also recorded at the quadpods, similar to that in Fig. 6.

The linked tidal variation in stratification, shear, and suspended sediment concentration was also apparent in the small-boat surveys of the tidal flats. Cross-flat surveys during spring tides found that after lower low tide the salinity gradient advancing across the flats during the flood was vertically well-mixed. Stratification developed on the upper flats around high water, and remained strong

through the early part of the strong ebb. An example of the cross-flat distribution of salinity, velocity, and acoustic backscatter during a strong ebb is shown (Fig. 4). During transect 1 early in the ebb, the stratified region extended across most of the tidal flats. Velocities were highly sheared near the surface due to the stratification and river outflow, with currents of about 0.5 m s^{-1} in the surface layer and near zero in the lower layer. About 1 hour later, the stratification had broken down on the upper flats but remained on the lower flats; correspondingly, the backscatter signal was strong where the water column was well mixed. The transition point during this survey occurred near station 2, and the instruments there showed a similar transition from strong stratification and low sediment concentrations to well-mixed with high suspended sediment. By transect 3, the well-mixed, high-backscatter region extended to the edge of the flats.

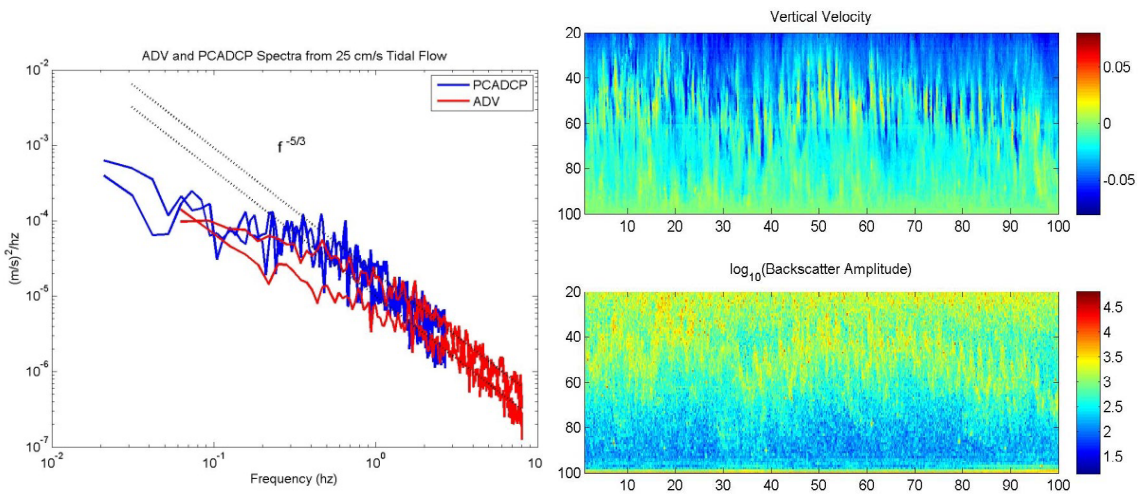

Figure 5. (left) Vertical velocity spectra from ADVs located at 25 and 75 cm and corresponding range bins of the multi-frequency pcADP. Both instruments show a similar $f^{-5/3}$ frequency dependence at high frequencies. (right) Color plots of vertical profiles of vertical velocity (top) and backscattered amplitude (bottom) reveal that the turbulence is associated with a series of high frequency internal waves. From the ADV data alone it would be difficult to distinguish turbulence generated solely from bottom friction from this combined mechanism.

In 2009 the recently developed multi-frequency acoustic pulse coherent Doppler profiler (pcADP) was deployed on the Skagit Tidal Flats, as well as in the Hudson River estuary. The multi-frequency processing was essential for using pulse coherent Doppler on the Skagit tidal flats as it allowed un-aliased velocities measurements in the 1 m/s flows present in the channels during spring ebb tides. The single frequency schemes at the same frequency, range and vertical resolution would have experienced aliasing at ±30 cm/s horizontal velocities, making for a difficult de-aliasing problem. Spectra of vertical velocity (Figure 5, left) show that the system is capable of producing high frequency $f^{-5/3}$ spectra similar to ADVs, although with a lower Nyquist frequency.. However; the combination of cm resolution profiles of vertical velocity and backscattered amplitude (Figure 5, right) showed additional structure that is not resolved the single sampling volume ADVs. Both the vertical velocity and the backscattered amplitude profiles had a series of 20 cm amplitude high frequency (~ 3 s) internal waves on an interface fluctuating 40 to 60 cm above the bed with a 20 to 60 s period. Vertical velocity

fluctuations were enhanced near the bed, thus the turbulence could have contributions from both bed friction and shear instabilities, which would not be easily detectable from the ADV data.

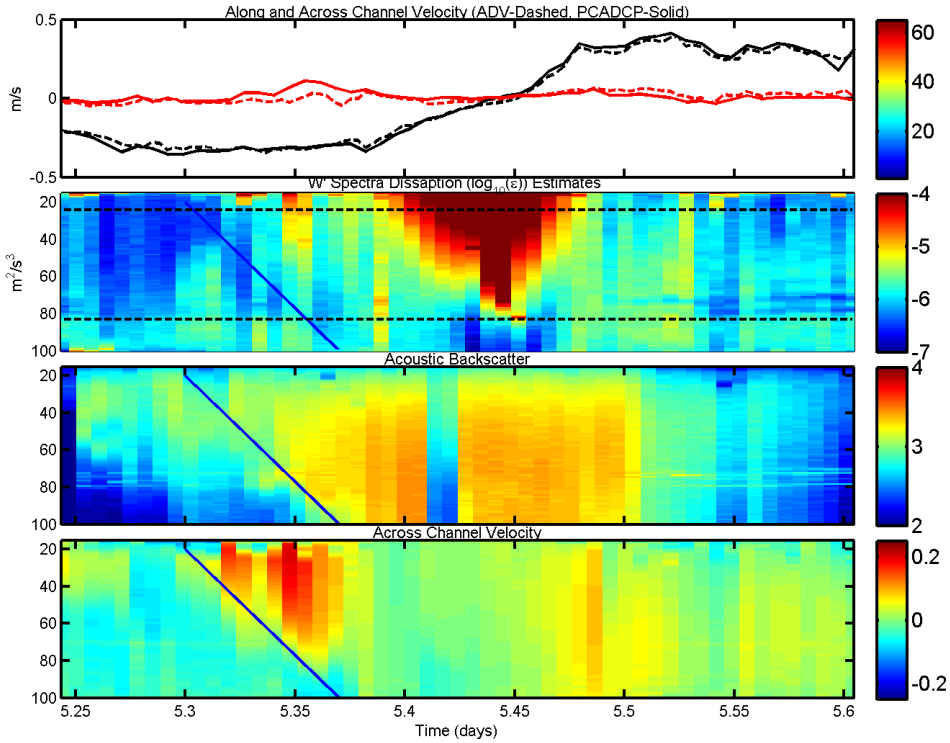

Figure 6. pcADP data from a Skagit tidal flats channel during the transition from ebb to flood. (top) Along channel (black, flood > 0) and across channel (red) horizontal velocity from the pcADP (solid) and an ADV (dashed). (panel 2) Estimates of turbulent dissipation calculated using the inertial dissipation method on vertical velocity spectra. The dissipation was low until the middle of ebb. At that time the salt wedge (blue diagonal line, e.g. see Figure 4 for cross-flats salinity structure), with a dissipation minima, advected past the profiler. (panel 3) Acoustic backscatter showed high scattering strengths above the salt wedge and toward the end of ebb as sediment is advected out the channel. (panel 4) Profiles of across channel velocity showed a flow reversal associated with the salt wedge as fresh sediment laden water from the flats flows laterally over salty water in the bottom of the channel.

Data from the lower channel station pcADP on the Skagit tidal flats taken during the transition from ebb to flood (Figure 6) shows the effects of near bed salinity stratification on the flow and turbulence structure. Estimates of turbulent dissipation, calculated using the inertial dissipation method on vertical velocity spectra, show weak turbulence as the ebb velocities increase. At the peak of ebb flow near bed turbulence increases, and there is a turbulence minima associated with a salt wedge that advents past the profiler from day 5.3 to 5.37. Acoustic backscatter shows high scattering strengths above the salt wedge and a flow reversal is evident in the lateral flow structure. This indicates sediment laden fresh water is flowing over clear salty water in the bottom of the channel. The stratification is sufficient to prevent resuspension of the sand in the channel during the peak of ebb. Once the salt wedge is advected past the profiler backscatter remains high until the peak of flood tide.

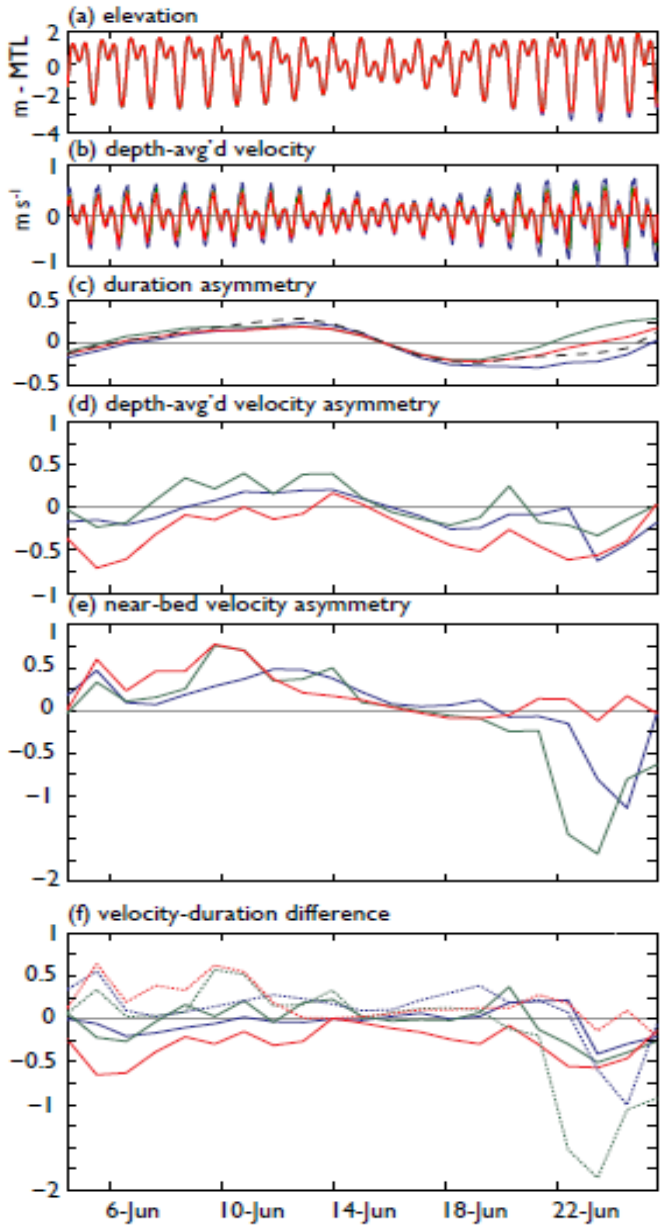

Figure 7: Asymmetry at station 1 (in channel, lower flats) [blue], station 5 (in channel, mid-flats) [green] and station 3 (outside channel, mid-flats) [red]. Positive asymmetry is flood-dominant, negative is ebb-dominant. (a) Water level, (b) depth-averaged velocity, (c) water level duration asymmetry, including Seattle tide gauge observations [black dashed], (d) observed depth-averaged velocity asymmetry (e) observed near-bed velocity asymmetry. Near-bed velocities are almost always flood dominant, the exception being at the channel stations (1 and 5) during extreme spring tides in the last week of the deployment when fluvial channelization becomes important. (f) difference between the tidal forcing (shown in panel c) and observed velocity asymmetry. Stratification and baroclinic forcing shift the tidal forcing (that varies in skewness over the spring-neap cycle) toward flood dominance.

Mechanisms of Tidal Asymmetry and Impacts on Sediment Transport

Tidal asymmetry in bottom stress and the duration of slack water often determine the net transport of sediment on tidal flats. However previous work on tidal asymmetry of tidal flats does not consider the combined influence of tides and freshwater discharge, which appears to be a dominant source of asymmetry on the Skagit flats. This freshwater discharge affects the asymmetry in 3 ways: 1) by augmenting the barotropic outflow (increasing ebb dominance, particularly in channels near low tide); 2) by increasing the baroclinic gradients (generally resulting in flood dominance due to the landward-directed bottom currents); and 3) by increasing stratification, which strongly influences bottom stress but may affect tidal asymmetry in either sense, depending on the timing of destratification. An additional source of asymmetry is the interaction of semidiurnal and diurnal astronomical constituents. This is particularly important in embayments connected to the Pacific Ocean, because of the comparable magnitudes of semidiurnal and diurnal constituents.

Data analysis suggests that tidal asymmetry depends on the tidal forcing, the stratification, and on the location on the tidal flats. In distribuary channels during big spring tides, the water column becomes unstatified around low water and net near bed flow is ebb dominant (Fig. 7). In contrast, during stratified neap tides and at locations removed from the distributary channels, the stress asymmetry is skewed toward flood dominance due to stratification and the baroclinic pressure gradient. The asymmetry also depends on the duration asymmetry in the tidal forcing that shifts on spring-neap and seasonal time scales in Puget Sound due to the mixed diurnal-semi-diurnal tides. The observational results are consistent with model simulations showing that the stratification and baroclinic pressure gradient at the tidal salinity front enhances near bed stress during flood tides and reduces bed stress during ebbs, leading to net landward sediment flux on unchannelized regions of the flats.

IMPACT/APPLICATIONS

Results from this project may be used to enhance morphological models of coastal regions near river mouths, with applications to environmental assessment for the Navy. Trapping and deposition of sediment associated with density fronts could introduce significant spatial and temporal variability in bed consolidation and bathymetric relief on tidal flats. The project will also help to evaluate the skill of coastal hydrodynamic models at resolving narrow density fronts, including the surface expression of such fronts that can be assessed with remote sensing observations.

RELATED PROJECTS

The work here is closely linked to several investigators in the Tidal Flat DRI. In particular, Ralston is PI on a closely related project entitled “Sediment transport at density fronts in shallow water”, which involves high resolution modeling of the hydrodynamics and sediment transport on the Skagit Flats using FVCOM. We have also shared data and discussed results with other investigators working on the Skagit, particularly the Raubenheimer and Elgar group at WHOI and Cowles at UMass Dartmouth. A post-doc (Nick Nidzieko at WHOI, currently at UMD Horn Point) worked with data from this project, although neither he was not directly funded by the project.

PUBLICATIONS

Ralston, DK, WR Geyer, PA Traykovski, and NJ Nidzieko, 2011. Effects of Estuarine estuarine and fluvial dynamics processes on sediment transport on over deltaic tidal flats, *Contintental Shelf Res.*, [submitted, refereed].

Nidzieko, NJ, and DK Ralston, 2011. Tidal asymmetry and velocity skew on an intertidal flat. *J. Geophys. Res.*, [submitted, refereed].